Original Article

MOLECULAR METABOLISM

# Physically interacting beta-delta pairs in the regenerating pancreas revealed by single-cell sequencing

**Eran Yanowski [1,2], Nancy S. Yacovzada [1,2], Eyal David [3], Amir Giladi [3], Diego Jaitin [3], Lydia Farack [4], Adi Egozi [4], Danny Ben-Zvi [5], Shalev Itzkovitz [4], Ido Amit [3], Eran Hornstein [1,2,*]**

## ABSTRACT

**Objectives:** Until recently, communication between neighboring cells in islets of Langerhans was overlooked by genomic technologies, which require rigorous tissue dissociation into single cells.
**Methods:** We utilize sorting of physically interacting cells (PICs) with single-cell RNA-sequencing to systematically map cellular interactions in the endocrine pancreas after pancreatectomy.
**Results:** The pancreas cellular landscape features pancreatectomy associated heterogeneity of beta-cells, including an interaction-specific program between paired beta and delta-cells.
**Conclusions:** Our analysis suggests that the particular cluster of beta-cells that pairs with delta-cells benefits from stress protection, implying that the interaction between beta- and delta-cells might safeguard against pancreatectomy associated challenges. The work encourages testing the potential relevance of physically-interacting beta-delta-cells also in diabetes mellitus.


**Keywords** Islet of Langerhans; Endocrine pancreas; Single-cell RNA-sequencing; Single-cell transcriptome sequencing; scRNA-seq; beta-delta cell pair; Pancreatectomy; Pancreas regeneration

## 1. INTRODUCTION

Pancreatic islets of Langerhans contain endocrine cells that are critical for regulating multiple aspects of metabolism. Beta- and alpha-cells, which release insulin and glucagon, respectively, are most abundant, whereas somatostatin-producing delta-cells are scarcer and act in a paracrine manner to inhibit the secretion of insulin and glucagon [1–3]. Additional endocrine cell types that express somatostatin receptors, such as pancreatic-polypeptide cells, might also be responding to somatostatin [4].

Several experimental paradigms were established for the study of pancreas regeneration in rodents, including injury models [5], pancreatic duct ligation [6], and chemical ablation of islet cells [7]. Partial pancreatectomy (Ppx) is a well-characterized experimental model for initiating endocrine and exocrine tissue regeneration. Regeneration peaks one week after pancreatectomy and animals regain euglycemia at about 4 weeks [8–11].

Much is known about beta-cell mass replenishment post partial pancreatectomy. New insulin-producing cells arise primarily from existing beta-cells that re-enter the cell division cycle [8,12]. In addition, auxiliary pathways commit beta-cells from other endocrine trajectories, including alpha- [13] and delta-lineages [14].

The SRY-Box Transcription Factor 9 (Sox9), plays a critical role in early pancreas development, giving rise to all three pancreatic compartments: duct, acinar, and endocrine [15]. However, during late embryogenesis, Sox9 expression becomes restricted to the predecessor of the ductal tree [16–19]. Overall, the potential contribution of the non-endocrine cells such as Sox9-descendants, to the regeneration of the endocrine pancreas was ruled out [18,20], with a notable recent observation that encourages further testing under certain experimental conditions [21].

Single-cell transcriptomics enables a new and thorough understanding of pancreas tissue dynamics and cellular heterogeneity [22]. Beta-cells display transcriptomic profiles associated with proliferation [23] and cellular stress [24,25]. Single-cell transcriptomics further revealed

[1]Department of Molecular Genetics, Weizmann Institute of Science, Rehovot 7610001, Israel [2]Department of Molecular Neuroscience, Weizmann Institute of Science, Rehovot 7610001, Israel [3]Department of Immunology, Weizmann Institute of Science, Rehovot 7610001, Israel [4]Department of Molecular Cell Biology, Weizmann Institute of Science, Rehovot 7610001, Israel [5]Department of Developmental Biology and Cancer Research, Institute for Medical Research Israel-Canada, The Hebrew University-Hadassah Medical School, Jerusalem, 9112102, Israel

*Corresponding author. Eran Hornstein, Department of Molecular Genetics, Weizmann Institute of Science, 234 Herzl St., 76100 Rehovot, Israel. E-mail: eran.hornstein@weizmann.ac.il (E. Hornstein).

*Abbreviations:* DIBs, Delta - Interacting Beta cells

Received October 24, 2021 • Revision received February 5, 2022 • Accepted February 25, 2022 • Available online 1 March 2022

https://doi.org/10.1016/j.molmet.2022.101467

 

molecular signatures typical of type 2 diabetes [26], post-pancreatectomy [27], and the aging organ [28].

In the current study, we apply single-cell transcriptomics to demonstrate that delta cells are Sox9-expressing cells that expand in the endocrine pancreas after partial pancreatectomy. We characterize pancreatectomy-associated beta-cell heterogeneity at a single-cell resolution and reveal molecular patterns that are consistent with the activation of stress programs in beta cells, or of the beta-cell division cycle. Furthermore, we identify a new type of interaction between beta and delta cells that is associated to a unique transcriptional profile. Exploring the crosstalk between endocrine cells in islets of Langerhans may contribute to a better understanding of how beta-cells cope with stress and to the development of therapies for injury and diabetes.

## 2. RESULTS

### 2.1. Islet Sox9-expressing cells are predominantly delta-cells

Sox9 plays critical roles in the development of the embryonic pancreas. However, in the adult organ it is predominantly expressed in the exocrine compartment. Accordingly, Sox9-descendant cells contribute to the ductal and acinar systems [19,29].

In an initial characterization of the Sox9-CreER:tdTomato allele [30], we observed a 12-fold increase, from 5% to 60%, in the expression of the tdTomato reporter in the exocrine compartment after tamoxifen induction, consistent with the broad activity of the Sox9 promoter in the exocrine compartment [18,29]. In addition we report a 3.6-fold increase in the tdTomato reporter expression in the endocrine pancreas, from 0.5% to 1.8%, after tamoxifen induction (Figs. S1A–D). These data quantify the activation (and degree of leakiness) of the Sox9-CreER knock-in allele in the exocrine and endocrine pancreas.

We next aimed to characterize which endocrine cell expresses the Sox9-CreER:tdTomato reporter within the islets of Langerhans (Figure 1A). Intriguingly, the islet cells that express the tdTomato reporter, primarily express the hormone somatostatin (Sst), which is typical of endocrine delta cells (Figure 1B–D). Quantification of the signal demonstrated that 78% of the tdTomato$^{+}$ cells are Sst$^{+}$, whereas 9% co-expressed insulin and 13% were neither delta nor beta-cells (Figure 1E, 1905 cells counted from 32 islets, obtained from five animals). Accordingly, 18% of the delta-cells were tdTomato$^{+}$, in contrast to only 0.4% of the beta-cell population (54 tdTomato$^{+}$and Sst$^{+}$/295 delta-cells and 6 tdTomato$^{+}$and Ins$^{+}$/1595 beta-cells Figure 1F). tdTomato was neither detected in alpha-cells, nor in intra-islet leucocytes (marked by Gcg and Cd45. Figs. S2A and B). These data suggest predominant expression of the Sox9-CreER knock-in allele in delta cells, within the endocrine pancreas.

To explore the nature of the tdTomato marked cells in additional molecular details, pancreata of 12 weeks old mice were dissociated into single cells and single-cell RNA sequencing analysis (MARS-seq protocol, as described in previous studies (31; 32)) was performed for both tdTomato$^{+}$ and tdTomato$^{-}$ cells. Transcriptional profile analysis identified five distinct cellular populations, namely beta-, delta-, gamma-, alpha- cells, and intra-islet leukocytes (Figure 1G–H). In addition, we identified a transcriptional signature that is typical of pairs of both beta- and delta-cells. These were therefore regarded as beta-delta doublet cells (cluster #1, Figure 1H). The expression of the tdTomato reporter was particularly enriched in delta-cells (Figure 1I), consistent with other analyses shown in Figure 1B–F. This might be either because of leaky tdTomato expression or due to delta cell-specific expression of the Sox9-CreER recombinase. We next demonstrated that the endogenous Sox9 is expressed rather specifically and is enriched in Sst + delta-cells (Fig. S3A). Furthermore, immunostaining revealed that ~ two-thirds of delta-cells co-express the protein SOX9 (Figs. S3B–D). Together, these analyses demonstrate that endogenous SOX9 is expressed in delta cells and provide a conceivable explanation for the activity of the Sox9-CreER:tdTomato allele in delta cells.

### 2.2. A single-cell map of the pancreatectomized islet

While the regenerative capacity of beta-cells gained a lot of attention [33,34], the response of delta-cells post-pancreatectomy is poorly investigated. Partial (subtotal) pancreatectomy (Ppx), was performed on 12 week-old Sox9-CreER; tdTomato males. Excision of ~70% of the pancreas was controlled by a cohort of sham-operated littermates. One week after surgery, beta-cell proliferation increased 6-fold and the number of islets with proliferating beta-cells increased 3-fold. Accordingly, blood glucose levels were monitored during the first 4 weeks after the surgical procedure (Figs. S4A–C). Therefore, as expected, beta-cell re-enters the cell division cycle and normoglycemia is gained 4 weeks after Ppx.

In addition, we observed a 1.5- to 2-fold increase in the number of delta cells 4 weeks after pancreatectomy, which is consistent with increased delta cell proliferation after Ppx, relative to sham-operated mice (Fig. S4D–M).

To investigate the cellular dynamics of pancreatic islets at a single-cell resolution following pancreatectomy, islets were dissociated from Sox9-CreER:tdTomato mice, four weeks after partial pancreatectomy. Islet cells were sorted by flow cytometry, in which tdTomato$^{+}$ cells were recorded, and single-cell RNA sequencing was performed (Figure 2A). Four endocrine cellular populations (alpha-, beta-, gamma-, and delta-cells), leukocytes, endothelial, and mesenchymal cells were detected (Figure 2B–D), consistent with the profile gained under basal conditions (illustrated in Figure 1).

Single-cell analysis revealed relative depletion of alpha cells in Ppx samples (only 20% originate from Ppx samples, 80% from sham samples), enrichment of gamma-cells (~80% originate from Ppx samples), and pancreatectomy-driven heterogeneity within the beta-cell population (Figure 2E).

### 2.3. Heterogeneity of beta-cells following partial pancreatectomy

Detailed analysis of beta-cell mRNA profiles revealed acquired heterogeneity in response to pancreatectomy. In addition to relatively-stable beta-cells that do not transcriptionally change in response to regeneration (Subset C, Figure 3A), beta-cells featured elevated levels of stress-associated transcripts (Fkbp11, Dapl1, Creld2, Sdf2l1, Pdia4 & Derl3; subset A, Figure 3A, B), whereas other beta cells have been denoted by cell-cycle-associated transcripts (e.g., Top2a, Ccna2, Ube2c, Cenpf & Nusap1; subset B, Figure 3A, C). The three signatures exhibited tonic expression of Ins1, but they could be further distinguished by discrete levels of Ins2 expression (Figure 3D). Thus, beta cells with stress-associated transcripts also express relatively low levels of Ins2 mRNA (Figure 3D, E). In summary, beta-cell heterogeneity increases in the pancreas after Ppx, denoting three primary transcriptional states: stress-associated, cell-cycle-associated, or basal state.

Overall, our data reveal previously overlooked cellular dynamics of the endocrine pancreas after Ppx, including relative alpha-cell depletion, relative gamma-cell enrichment, and considerable beta-cell heterogeneity.

### 2.4. Physically interacting beta-delta cell pairs

We unexpectedly identified a relatively large number of beta-delta pairs and alpha–delta pairs, which is atypical for MARS-seq data (MARS-

 

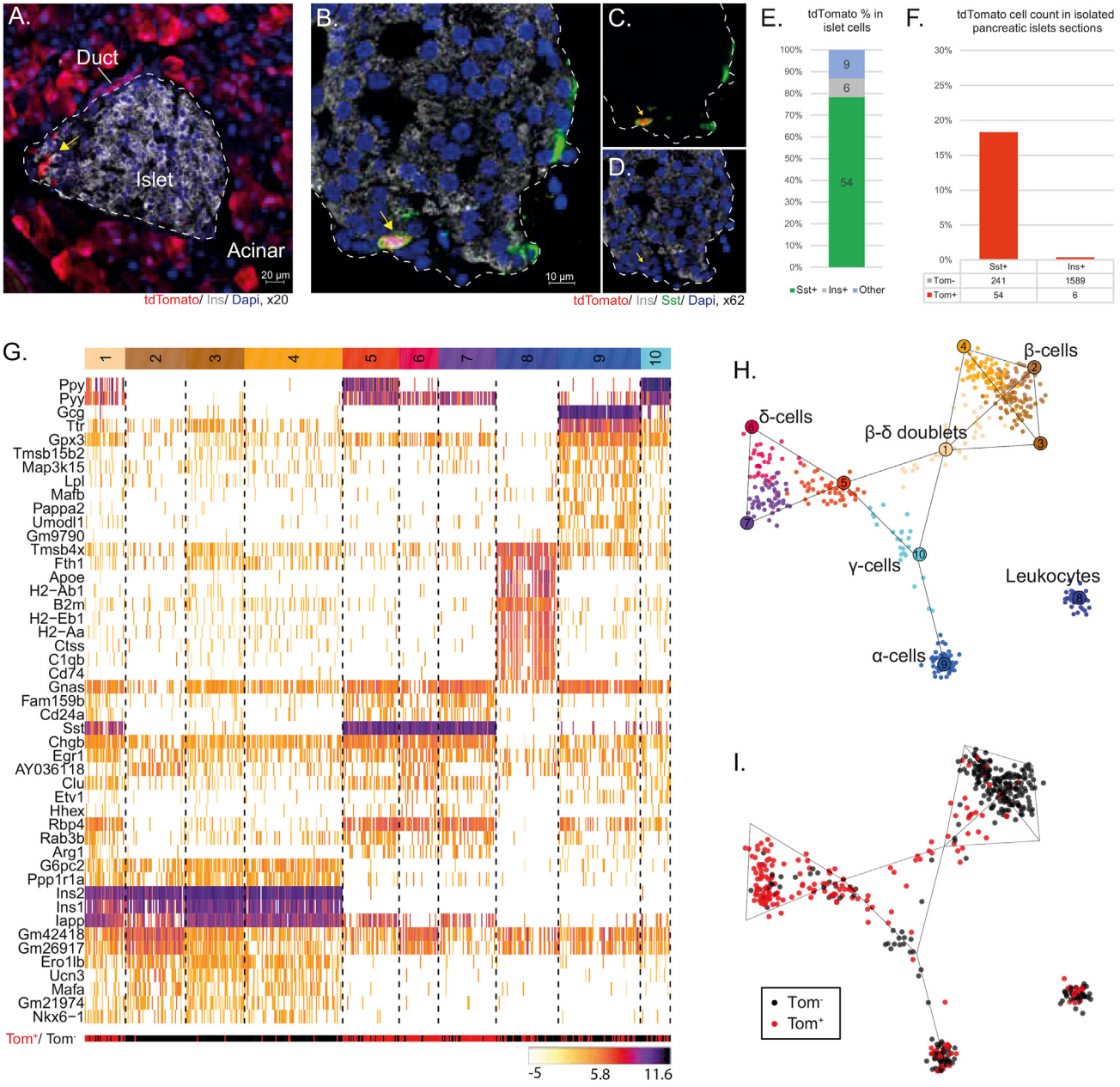


**Figure 1: Delta-cells are Sox9 expressing cells**. Confocal micrographs demonstrating that **(A)** Sox9 lineage tracing marks duct and acinar cells and cells at the periphery of Islets of Langerhans (Marked by yellow arrow). Islet border is marked by a white dashed line. **(B)** Sst + delta-cells are Sox-9 expressing cells. tdTomato signal (red, yellow arrow), insulin (white) Sst (green) and nuclei (blue) co-staining in four channels, or inset with two channels **(C, D)**. The Islet border is marked by a white dashed line. **(E)** Quantification of tdTomato + fractional enrichment in endocrine populations: delta-cells (78%), beta-cells (9%) or other islet cells (13%). Numbering on bars indicates the number of cells recorded. **(F)** 20% of Sst + cells (54 of 295 cells) and ~0.4% of Ins + cells (6 of 1595 cells) are Sox9-expressing cells (tdTomato+). **(G)** Heatmap of unsupervised clustering of single endocrine cell transcriptome from 590 dissociated cells of 6 pancreata of Sox9 lineage-traced pancreata. Analysis reveals that Ppy, Pyy, and Sst mRNAs are enriched in lineage traced tdTomato + cells (bottom red/black bar). Ten key cell type clusters are coded by a spectral bar. The bottom scale bar indicates signal intensity as log of (normalized UMIs). **(H)** Dimensional reduction of transcriptomic data, with cell-types spectral color, corresponding to Figure 1G. **(I)** Color-coded tdTomato-expressing cells (red) or cells unlabeled with tdTomato during the course of the experiment, superimposed on the dimensional reduction map, highlights the enrichment of Sox9-expressing delta-cells.

seq2.0 [35]). We sought to establish whether these pairs are indeed genuine doublets.

Because the typical number of transcripts is significantly larger in the presumed pairs than in any single endocrine cell type, we excluded the possibility of a polyhormonal phenotype (Tukey's multiple comparisons test of unique molecular identifier (UMI) distribution, p-value $<0.0001$, Figs. S5A and B).

In addition, the transcriptome of beta-delta pairs is predominated by beta-cell mRNAs, consistent with a beta-delta cell size difference (Fig. S5C), and therefore it is unlikely to be gained only from delta-cells, contaminated by cell-free RNA from fragmented beta-cells.

We demonstrated that the pairing of delta to beta-cells is specific and is significantly enriched, relative to other endocrine cell couples (randomization permutation test, 10,000 iterations, $p < 0.0001$). Thus

 

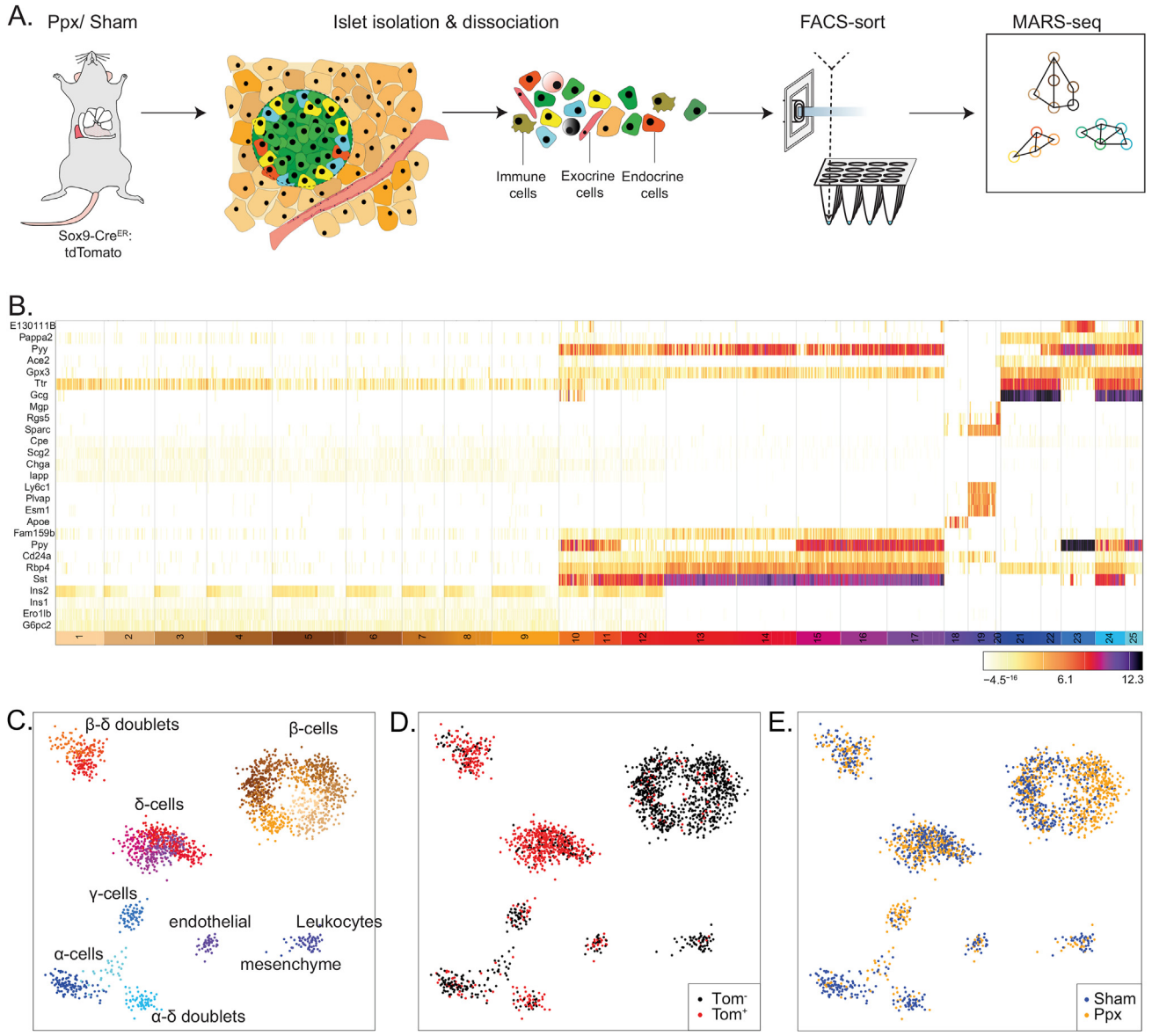


**Figure 2: Single-cell map of the pancreatectomized islet. (A)** Diagram of the experimental setup for single-cell RNA sequencing of endocrine cells from the regenerating pancreas. **(B)** Heatmap of clustered islet cells RNA-sequencing data from 2300 cells collected from Sox9 lineage-traced 6 pancreata, 4 weeks after partial pancreatectomy. Sham-operated mice and pancreata without lineage tracing were included in the same analysis. Meta-cells (columns) and maximally enriched gene markers (rows) were analyzed as in [32]. **(C)** Two-dimensional projection of Meta-cells and inferred cell-types. **(D)** lineage traced Sox9-expressing cells (tdTomato, red) and **(E)** cell source from sham-operated (blue) or regenerating pancreata (orange).

beta-delta pairs are observed more than can be expected at random and are unlikely to result from cell—cell adhesion in the tube after dissociation.

Next, we simulated *in silico* synthetic doublets, by summing the transcriptome of beta-and delta cells (Figs. S6A and B). The gained synthetic transcriptome differs from real doublets in the expression of 21 mRNAs that are expressed $>$ 2-fold in real pairs relative to simulated pairs ($\chi^2$ statistics, adjusted p-value $<$ 0.01, (Fig. S7). mRNAs enriched in doublets more than expected include Dock3, a regulator of cytoskeletal organization and cell—cell interactions [36—38], and several transcription factors of the zinc finger protein family [39]. Overall, this study reveals genuine pairs of beta- and delta-cells in the endocrine pancreas.

### 2.5. Delta cells interact with particular beta-cell types

Several studies have described physical interactions of delta cells with adjacent alpha- or beta-cells in the tissue [2,40,41]. We sought to evaluate the nature of physically interacting beta—delta conjugates using PIC-seq, an analytical pipeline for physically interacting cells [42]. PIC-seq allows deconvoluting heterotypic cellular pairs, by assigning to each paired-cell the transcriptional identity of its contributing partners, based on a background singlet model. The PIC-seq algorithm receives as input a genes-over-cells expression matrix of the paired cells and two background profiles of non-conjugated single-cell populations. In addition, it assigns a meta cell identity for every single cell from the given population. Thus, each PIC can be described as a linear mixture of two cells [42].

 

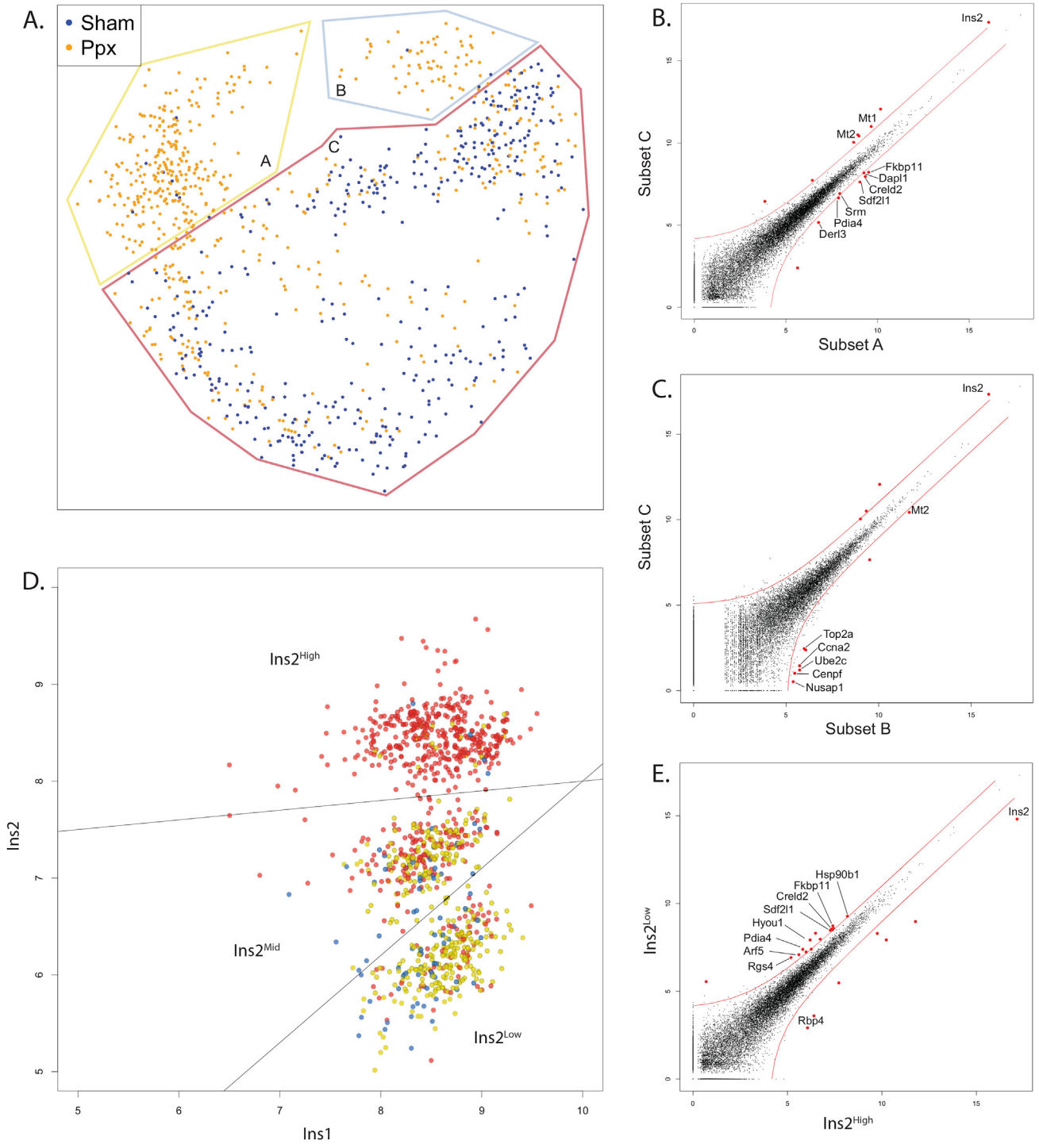


**Figure 3: Heterogeneity of beta-cells following partial pancreatectomy. (A)** Dimension reduction map depicting beta-cell heterogeneity after regeneration with enrichment of two subsets (a, orange; b, blue) and a single subset that persists in basal conditions (c, red). Scatter plots of differential mRNA expression between beta-cell subsets highlights enrichment of stress-related mRNAs (**B**, subset a vs. c) and cell-division-cycle mRNAs (**C**, subset b vs. c) in regeneration. **(D)** Scatter plot of 974 beta-cells, scattered according to their Ins2 mRNA levels (y-axis) versus Ins1 mRNA levels (x-axis). Log2 of read counts. Cells from sham control and after Ppx. Cells (dots) colored according to subsets in Figure 3A. **(E)** Differential mRNA expression between beta-cells that express low and high levels of Ins2 mRNA. Unique molecular identifier (UMIs) normalized to total reads and to cell numbers.

PIC-seq characterized pure beta- or delta-cellular subsets (Figure 4A–E), and a joint signature of beta-delta pairs (Figure 4F). The relative contribution of beta- and delta-cell mRNAs to the superimposed profile (Figure 4G), was consistent with 20,000 synthetic simulated delta-beta pairs and with the UMI-count differences between the two cell types (Fig. S8A–D).

Unexpectedly, among the different subtypes of beta cells, one particular beta-cell subset interacted with delta cells. Hence, these were

 

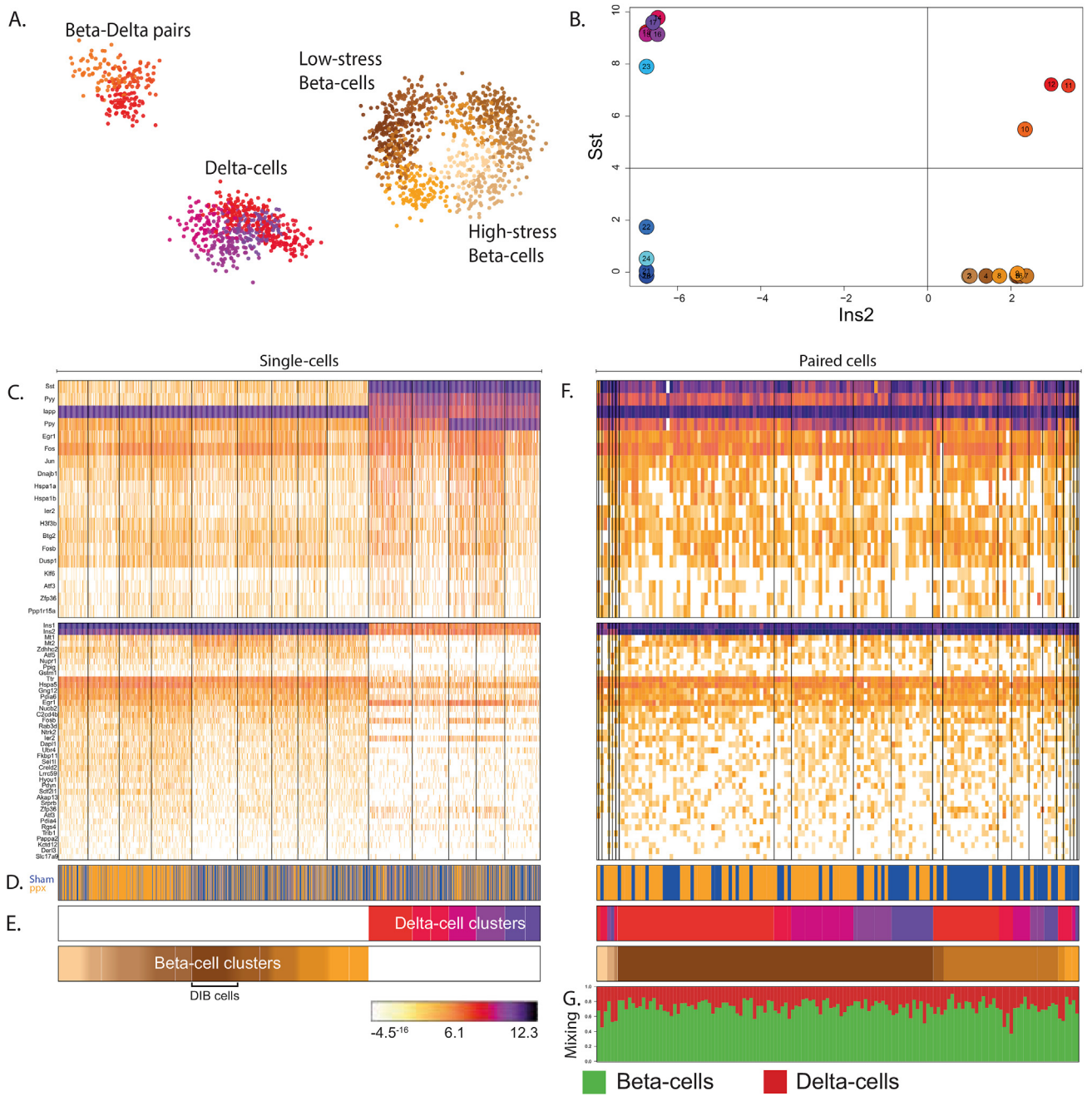


**Figure 4: Physically interacting beta-delta cell pairs. (A)** Two-dimensional projection of beta-cells, delta-cells, and beta-delta cell pairs. **(B)** Scatter-plot of 14 cellular subsets, demonstrating the identification of pure beta- or delta-cell, by Ins2, or Sst and a joint signature with high expression of both hormones (subsets 10,11,12). **(C)** Heatmap of clustered RNA-sequencing data, 4 weeks after partial pancreatectomy, defines 9 beta-cell subsets and 5 delta-cell subsets. Upper and lower panels indicate identity genes in delta- and beta-cell clusters, respectively. Data of 1500 cells collected from 6 pancreata analyzed by MetaCell [32]. Sham-operated mice and mice lacking lineage tracing were included in the same analysis. Meta-cells (columns) and maximally enriched gene markers (rows). Color-bar indicators of **(D)** partitioning of cells derived from sham (blue) or Ppx (orange) pancreata or **(E)** beta/delta meta-cells. Int-beta are interacting beta-cells. The bottom scale bar indicates log (normalized UMIs). **(F)** Heatmap of clustered RNA-sequencing data, of 212 physically interacting beta-delta cell pairs, grouped by their contributing beta- and delta-cell identities. **(G)** Annotation and estimation of relative transcriptome contribution, derived from beta/delta cells (green/red).

dubbed Delta-Interacting Beta-cells (DIBs). DIBs typically express high levels of beta-cell function gene (Ins2, Mt1, Mt2, Zdhhc2, Atf5, Nupr1, Ppig, and Gstm1) and low levels of unfolded protein response (UPR)-associated genes (Hap5a, Pdia6, Fkbp11, etc.). A study of the DIB transcriptome reveals that it is reminiscent neither of immature "virgin" beta-cells [13] nor of replicating beta-cells [43]. Furthermore, proliferating beta cells (Ki67$^{+}$) are preferentially positioned distant from delta cells (Fig. S8E). Therefore, DIBs display a molecular

 

fingerprint of non-proliferating and highly functional beta cells and suggest that interactions with delta cells may be beneficial for beta cells, which are coping with tissue or metabolic challenges, imposed by injury or regeneration.

### 2.6. Beta-cells, juxtaposed to delta-cells, display a specific molecular signature

To validate the single-cell sequencing results, we orthogonally performed a single-molecule fluorescence *in situ* hybridization (smFISH) study for the detection of Sst and Ins2 (Figure 5A—C). Approximately 23% of the beta cells in the endocrine pancreas reside at the proximity of delta cells in sham or pancreatectomized mice, consistent with a previous study [40]. Of these, DIBs phenotype was denoted in 31.3% of beta-delta pairs after Ppx, compared to 13.4% of the sham-operated controls.

In addition, we studied stress-related Fkbp11 mRNA, which was suggested by the single-cell sequencing to be one of the markers of stressed beta-cells (Figure 3). The quantification revealed that beta-cells juxtaposed to delta-cells, express lower levels of Fkbp11 mRNA and higher levels of Ins2 mRNA, relative to beta-cells distant from delta-cells in the pancreatectomized pancreas, and relative to beta-cells that are paired to delta-cells under non-regeneration basal conditions (Figure 5D,E, quantification of smFISH signal in 1361 cells, derived from 16 islets / 6 pancreata. non-parametric Kolmogorov—Smirnov test). These studies resonate with the initial conclusion that DIBs display the molecular fingerprint of highly functional and relatively unstressed beta cells.

Finally, we conducted immunostaining with an antibody raised against musculoaponeurotic fibrosarcoma oncogene homolog A (MAFA), whose protein levels correlate with beta-cell function [44—46]. DIBs held higher levels of MAFA, following pancreatectomy, relative to beta cells distant from delta cells or beta cells in sham-operated animals (Figure 5F—J).

Overall, considering several orthogonal approaches we suggest that beta-cells that are at physical interaction with delta-cells exhibit reduced stress signature and elevated functional profile, after pancreatectomy.

## 3. DISCUSSION

The emergence of single-cell transcriptome profiling paves the way to studies of endocrine pancreas heterogeneity at unprecedented cellular resolution. The current study portrays the cellular status of the endocrine pancreas after surgical resection. It resonates with some of the observations reported by Tatsuoka et al. [27], where self-duplicating beta-cells were observed following partial pancreatectomy. Our work further offers a new look into beta-cell heterogeneity following pancreatectomy and reveals physically interacting endocrine cells, which were overlooked until the recent development of computational methods for discrimination of true interactions from doublet artifacts.

Additionally, we report that following partial pancreatectomy there is a relative reduction in alpha-cell populations, accompanied by a relative expansion of gamma-cells. In addition, the beta-cell population diversifies. Thus, pancreatectomy-associated beta-cell heterogeneity appears to progress three-fold: some beta cells feature ER-stress-associated markers (e.g., Fkbp11, Dapl1, Creld2), cell division cycle markers (e.g., Top2a, Ccna2, Ube2c), or beta-cell activity markers (high Ins2 along with Mt1, Mt2, ATF5, and Nupr1), accompanied with low UPR stress markers.

We further document the unexpected dynamics in the delta-beta axis. We demonstrate that delta-cells can be denoted by the activation of a lineage tracer that is driven by the endogenous promoter of the transcription factor Sox-9. It is noticeable because in the mature organ, Sox9 is primarily expressed in ductal and centero-acinar cells [17,19,47]. However, a careful analysis reveals the expression of endogenous Sox9 mRNA and protein and suggests that these Sox9-expressing cells are most likely intrinsically endocrine. Furthermore, we did not find any evidence in support of an alternative explanation, making it a less likely interpretation that the Sox-9 descendants might be of non-endocrine origin.

Beta-cells re-enter the cell division cycle in the regenerating pancreas, peaking at the first week after injury [12,48—50] and were recently suggested to be associated with intricate activation of the stress response, cell cycle progression effectors, and tumor suppressors [27]. Our analysis reveals residual replication of beta-cells, even 4 weeks following surgery, indicative of a replication phase that is prolonged relative to previous reports [48].

We demonstrate an increase in the fraction of beta cells that interact with delta cells after pancreatectomy. In part, this can be associated with delta cell proliferation, following pancreatectomy, and is consistent with delta-cell hyperplasia in rodent diabetes models [51,52].

We demonstrate that DIBs display broad transcriptomic differences with reference to other beta-cell subsets. However, it is unknown whether the physical interaction with delta cells imposes these transcriptional changes to beta-cells and/or that only specific subtypes of beta-cells are molecularly competent to induce beta-delta interactions.

Beta-delta cell proximity and cellular crosstalk were previously described [2,40,51,53], but were not systematically quantified in the pancreas after pancreatectomy. The current study suggests that beta-cell physical interaction with delta cells is associated with reduced expression of stress markers and with augmented expression of mRNAs and proteins typical of beta-cell function. These two entities may be linked by the fact that the high demand for insulin secretion imposes stress on beta-cells [54].

In summary, we suggest that physically interacting delta cells provide a unique protective niche that safeguards beta-cells from exhaustion in the event of prolonged hyperglycemia or following pancreas injury. However, it remains undefined if paracrine somatostatin or other means of cellular communication play a role in establishing this protective function. Finally, it would be important to test the potential relevance of physically interacting beta-delta-cells also in other contexts, including in models of diabetes mellitus.

## 4. LIMITATIONS

The study is the first to perform an analysis of cellular pairs in the endocrine pancreas. However, the functional importance of beta-delta crosstalk requires additional studies. Plausibly, paracrine somatostatin plays a role in controlling beta-cell transcriptome and function. However, non-secreted membrane-bound molecules might be additionally considered as means of communication. Our study focuses on a defined time point, 4 weeks after pancreatectomy, encouraging detailed future studies of the dynamics of beta-delta pairing in earlier phases of regeneration and in additional clinically-relevant models of diabetes.

Delta cells extend compound filopodia-like protrusions to communicate with cells in their vicinity [40]. Therefore, a quantified pairing of beta- and delta-cells by microscopy and taking into account the potential of delta cells to affect beta-cells that are considered by our calculation as

 

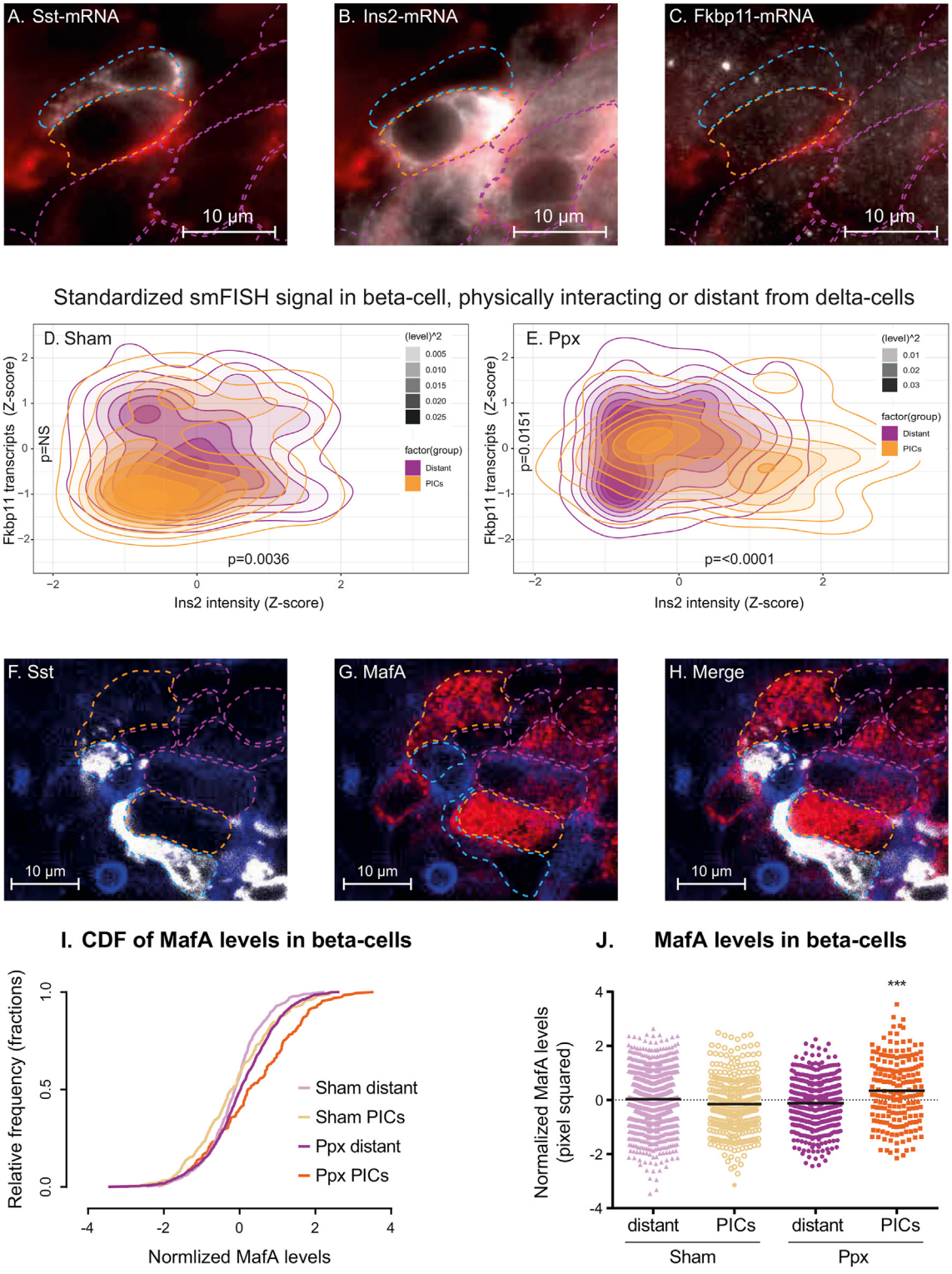


**Figure 5: Functional relevance of physically interacting beta-cells following pancreatectomy.** SmFISH study micrographs of Sst (**A**), Ins2 (**B**), and Fkbp11 (**C**) mRNAs in islets of Langerhans. Beta-cells, juxtaposing delta-cells (orange), beta-cells distant from delta-cells (purple), and Sst+ delta-cells (blue). Cell membrane demonstrated by Phalloidin staining (red), smFISH signal (white). Density map of standardized Fkbp11 mRNA (y-axis) vs. Ins2 mRNA (x-axis) in 1361 cells, derived from 16 islets/6 pancreata. Beta-cells, juxtaposing delta-cells (orange, PICs) and beta-cells distant from delta-cells (purple), in islets from sham-operated mice (sham, **D**) or following pancreatectomy (Ppx, **E**). Data gained by quantification of smFISH signal in 1361 cells, derived from 16 islets / 6 pancreata. P-values were calculated using non-parametric Kolmogorov–Smirnov test (between distant vs. PICs for Fkbp11 and Ins2 transcript levels. Immunostaining confocal micrographs demonstrating **(F)** Sst and **(G)** MafA protein levels, in islets of Langerhans (merged channels in **H**). Beta-cells, juxtaposing delta-cells (orange), beta cells distant from delta-cells (purple), and Sst+ delta-cells (light blue). Cell membrane demonstrated by Phalloidin staining (blue). **(I)** A cumulative distribution function plot or **(J)** a scatter plot of standardized MafA levels in beta-cells from sham or Ppx mice (4 weeks recovery), neighboring (PICs), or distant from delta-cells. Data gained by quantification of immuno-fluorescent signal in 2589 cells, derived from 43 islets / 4 pancreata. P-values calculated by non-parametric Kolmogorov–Smirnov test (between distant vs. PICs).

 

'distant, non-interacting beta-cells', might underestimate the real effect of beta-delta pairing events.

Overall, the cellular composition of the pancreatectomized endocrine pancreas is unfolded by single-cell sequencing. Pancreatectomy-associated heterogeneity of beta-cell is suggested to involve physical interactions with delta-cells that attenuate the load of stress and plausibly enable a more robust beta-cell function. This may potentially involve suppression of beta-cell secretory activity, by SST and/or SST-independent mechanism.

## 5. METHODS

### 5.1. Animal experiments

Animal experiments were approved by the Institutional Animal Care and Use Committee of the Weizmann Institute of Science, Israel. Mice were housed in a specific pathogen-free facility in individually ventilated cages on a strict 12-h light–dark cycle. C57BL/6 strain was purchased from Envigo. For lineage tracing, Sox9-Cre $^{ERT2}$ mice [30] were crossed on to R26R-tdTomato conditional reporter [B6; 129S6-Gt (ROSA)26Sortm9(CAG-tdTomato)Hze/J [55]]. 10 weeks old Sox9-Cre$^{ERT2}$;tdTomato males were injected subcutaneously with tamoxifen (diluted in corn-oil, 0.2–0.4 mg tamoxifen (T5648, Sigma Aldrich) per gram body weight. mice body weight ~20–25 gm). Full clearance of residual tissue tamoxifen was allowed over 14 days, before any additional procedure. Subtotal surgical resection of the pancreas (partial pancreatectomy) was performed on isoflurane-anesthetized 12-week-old male mice, via midline abdominal incision, removing ~70% of the pancreas tissue, while preserving the pancreatic duct and splenic artery. Sham laparotomy and minimal rubbing of the pancreas with sterile q-tips served as the control procedure. Abdominal muscles and skin were sutured using absorbable PGA 5/0 sutures (Intrag Medical Techs Co/Ltd.). Further, 0.1 mg/kg buprenorphine-HCl in normal saline was injected subcutaneously for analgesia, and enrofloxacin (2 ml/400 ml) was given as a prophylaxis oral antibiotic in drinking water for 7 days.

### 5.2. Tissue microscopy

Islets of Langerhans were isolated by retrograde intra-ductal perfusion of pancreata with 5 ml 0.8 mg/ml Collagenase-P following the protocol described in [56]. Freshly isolated islets of Langerhans or whole pancreata were fixed in 4% paraformaldehyde (PFA)/PBS at 4 °C overnight, dehydrated in 30% sucrose, soaked in OCT (Tissue-Tek), frozen in mold on dry ice. Cryosections of 8 μm (Cryostat M3050S, Leica) were mounted onto Superfrost plus slides. For immunofluorescence, cryosections were airdried for 30 min, permeabilized with 0.2% Triton/TBS, incubated with Cas-block (008120 Thermo Fisher) for 10 min and then incubated overnight at 4 °C with primary antibodies, diluted in CAS-block. Sections were washed in PBS and incubated with secondary fluorescent antibody, mounted on glass slides with DAPI-mounting medium (Fluoroshield™ with DAPI, Sigma). Slides were air-dried overnight and examined with LSM 800 laser-scanning confocal microscope (Carl Zeiss), equipped with a Zeiss camera with × 20/x40 or × 63 magnification (Thornwood, NY, USA). The following primary antibodies were used: guinea-pig anti-INS (ab7842; Abcam, 1:200), goat anti-SST (SC-7819; Santa Cruz biotechnology, 1:200), rabbit anti-MAFA (A300-611A; Thermo Scientific, 1:200), goat anti-GCG (sc-7780; Santa Cruz, 1:200), rabbit anti-KI67 (RM-9106-S1; Thermo Scientific, 1:200) or rabbit anti-SOX9 (AB5535; Millipore, 1:200). All antibodies were previously validated, and immunostaining included negative controls (no primary antibody). Single-Molecule FISH was performed as described previously [57–59] using Stellaris FISH Probe libraries (Table 1. Biosearch Technologies, Inc., Petaluma, CA, USA), coupled to Cy5 (GE Healthcare, PA25001), Alexa594 (Thermo Fisher, A37572) or TMR (Molecular Probes, C6123). Wash buffer and hybridization buffer contained 30% Formamide. Nuclei were counterstained with DAPI (Sigma–Aldrich, D9542) and cell borders, counterstained with Alexa fluor 488-conjugated phalloidin (Thermo Fisher, A12379). The slides were mounted using ProLong Gold (Molecular Probes, P36934). Endocrine cells were detected by insulin or somatostatin signals. Micrographs captured by Nikon inverted fluorescence microscope eclipse ti2 series, equipped with a 100 × oil-immersion objective and Ixon ultra 888 camera using NIS elements advanced research (Nikon). The image-plane pixel dimension was 0.13 μm. Quantification was performed on stacks of five optical sections, at 0.3 μm intervals, in which not more than a single cell was observed.

### 5.3. Endocrine single-cell studies

Isolated Islets of Langerhans were dispersed to single-cell suspensions by incubation in a solution of 50% trypsin–EDTA (GIBCO) at 37 °C for 3 min followed by gentile mechanic agitation and stopped by adding 10% RPMI 1640/FBS (vol/vol). For cell sorting, islet cells were suspended in ice-cold sorting buffer (PBS supplemented with 0.2 mM ethylenediaminetetraacetic acid, pH 8 and 0.5% BSA), filtered through a 50-μm cell strainer, and stained for viability by DAPI (1 ug/ml). Flow cytometry analysis and sorting were performed on a BD FACSAria Fusion instrument (BD Immunocytometry Systems), using a 100 μm nozzle, controlled by BD FACS Diva software v8.0.1 (BD Biosciences). Further analysis was performed using FlowJo software v10.2 (Tree Star). Either unstained, single-stained tdTomato, or DAPI only control cells were used for configuration and determining gates boundaries. tdTomato$^{+}$/DAPI$^{-}$ target cells were sorted into 384-well cell-capture plates containing 2 μl lysis solution and barcoded poly(T) reverse-transcription primers for single-cell RNA-seq. Empty wells in the 384-well plates served no-cell controls. Immediately after sorting, each plate was spun down to ensure cell immersion into the lysis solution, and frozen at −80 °C until processed. Single-cell libraries cDNA were prepared (reverse-transcribed) from mRNA of islet cells barcodes [31,35]. Single-cell RNA-seq (scRNA-seq) libraries were

**Table 1** – Stellaris probe libraries used in smFISH studies.

| Probe # | Sst | Ins2 |
|---|---|---|
| 1 | Tcggtagcgtctccttcagc | ctggtggttactgggtcccc |
| 2 | Tcctcaggcagcagcgacgg | gattgtagcggatcacttag |
| 3 | Cagccagggcgcactggaga | ttcctgcttgctgatggttt |
| 4 | Aaagccaggacgatgcagag | aacaataacctggaagatag |
| 5 | Aactgacggagtctggggtc | cgcatccacagggccatgtt |
| 6 | Agccgccagagacttctgca | cagggccagcaggggcagga |
| 7 | Ccagttcctgtttcccggtg | ggtgggactcccagaggaag |
| 8 | agctctgccaagaagtactt | tgcttgacaaaagcctgggt |
| 9 | tgtctggttgggctcggaca | caggtgggaaccacaaaggt |
| 10 | cgggctccagggcatcattc | ccacttcacggcgggacatg |
| 11 | ctccagcctcatctcgtcct | agttgtgccacttgtgggtc |
| 12 | ttcgagttggcagacctctg | tcccgggcctccacccagct |
| 13 | ttcccggggtgccattgctg | ccaaggtctgaaggtcacct |
| 14 | agttcttgcagccagctttg | ttctgctgggccacctccag |
| 15 | gatgtgaatgtcttccagaa | agcactgatctacaatgcca |
| 16 | acaacaatattaaagctaac | taggctgggtagtggtgggt |
| 17 | agggatcagaggtctggcta | ggttttattcattgcagagg |
| 18 | agagatatggggtttggggg | |
| 19 | atcgggggccaggagttaag | |
| 20 | ctaatgcagggtcaagttga | |
| 21 | ttgtatttacagtcttcaat | |
| 22 | ataatctcaccataatttta | |

 

pooled at equimolar concentrations and sequenced on an Illumina NextSeq 500 at a median sequencing depth of 24,500 reads per cell. The sequences were mapped to the mouse genome (10 mm) using HISAT2 [60], demultiplexed, and filtered to exclude reads outside exons or with multiple mapping positions. Cell libraries with 500 - 500,000 UMIs and $<$20% mitochondrial mRNAs were included in downstream MetaCell analysis [32], which derives cohesive groups of cellular profiles. To study physical interaction between cells, we employed PIC-seq [42] on single-cell data.

## DATA AVAILABILITY

RNA-seq data that support the findings of the present study are deposited in the Gene Expression Omnibus under accession code GSE183788.

## CONFLICT OF INTEREST

The authors declare that they have no conflict of interest. Dr. Eran Yanowski is the guarantor of this work and, as such, had full access to all the data in the study and takes responsibility for the integrity of the data and the accuracy of the data analysis. Eran Hornstein is the corresponding author.

## ACKNOWLEDGMENTS

E.Y researched data and wrote the manuscript. N.S.Y and A.G PICseq computational analysis. E.D MARSseq computational analysis. D.J single-cell library preparation. L.F and A.E consultant smFISH. D.B.Z partial pancreatectomy training.
The work was funded by European Research Council under the European Union's Seventh Framework Programme (FP7/2007–2013)/ERC grant agreement 617351 and the Israel Science Foundation (135/16, 3497/21 and Legacy Morasha program 828/17); Research in the Hornstein lab is further supported by Radala Foundation; Minerva Foundation with funding from the Federal German Ministry for Education and Research, ISF Yeda-Sela, Yeda-CEO; Benoziyo Center Neurological Disease; Weizmann - Brazil Center for Research on Neurodegeneration at The Weizmann Institute of Science, Vener New Scientist Fund; Julius and Ray Charlestein Foundation; Fraida Foundation; Wolfson Family Charitable Trust; Abney Foundation; Merck; Maria Halphen and the estates of Fannie Sherr, Lola Asseof, Lilly Fulop, and E. and J. Moravitz, Redhill Foundation — Sam and Jean Rothberg Charitable Trust, Andi and Larry Wolfe Center for Neuroimmunology and Neuromodulation and by Dr. Sydney Brenner and friends.

## APPENDIX A. SUPPLEMENTARY DATA

Supplementary data to this article can be found online at https://doi.org/10.1016/j.molmet.2022.101467.

## REFERENCES

[1] Strowski, M.Z., Parmar, R.M., Blake, A.D., Schaeffer, J.M., 2000. Somatostatin inhibits insulin and glucagon secretion via two receptors subtypes: an in vitro study of pancreatic islets from somatostatin receptor 2 knockout mice. Endocrinology 141:111–117.

[2] Briant, L.J.B., Reinbothe, T.M., Spiliotis, I., Miranda, C., Rodriguez, B., Rorsman, P., 2018. delta-cells and beta-cells are electrically coupled and regulate alpha-cell activity via somatostatin. Journal of Physiology 596:197–215.

[3] Alberti, K.G., Christensen, N.J., Christensen, S.E., Hansen, A.P., Iversen, J., Lundbaek, K., et al., 1973. Inhibition of insulin secretion by somatostatin. Lancet 2:1299–1301.

[4] Ludvigsen, E., Olsson, R., Stridsberg, M., Janson, E.T., Sandler, S., 2004. Expression and distribution of somatostatin receptor subtypes in the pancreatic islets of mice and rats. Journal of Histochemistry and Cytochemistry 52:391–400.

[5] Bonner-Weir, S., Baxter, L.A., Schuppin, G.T., Smith, F.E., 1993. A second pathway for regeneration of adult exocrine and endocrine pancreas. A possible recapitulation of embryonic development. Diabetes 42:1715–1720.

[6] Xu, X., D'Hoker, J., Stange, G., Bonne, S., De Leu, N., Xiao, X., et al., 2008. Beta cells can be generated from endogenous progenitors in injured adult mouse pancreas. Cell 132:197–207.

[7] Fernandes, A., King, L.C., Guz, Y., Stein, R., Wright, C.V., Teitelman, G., 1997. Differentiation of new insulin-producing cells is induced by injury in adult pancreatic islets. Endocrinology 138:1750–1762.

[8] Lee, C.S., De Leon, D.D., Kaestner, K.H., Stoffers, D.A., 2006. Regeneration of pancreatic islets after partial pancreatectomy in mice does not involve the reactivation of neurogenin-3. Diabetes 55:269–272.

[9] Jonas, J.C., Laybutt, D.R., Steil, G.M., Trivedi, N., Pertusa, J.G., Van de Casteele, M., et al., 2001. High glucose stimulates early response gene c-Myc expression in rat pancreatic beta cells. Journal of Biological Chemistry 276:35375–35381.

[10] Laybutt, D.R., Weir, G.C., Kaneto, H., Lebet, J., Palmiter, R.D., Sharma, A., et al., 2002. Overexpression of c-Myc in beta-cells of transgenic mice causes proliferation and apoptosis, downregulation of insulin gene expression, and diabetes. Diabetes 51:1793–1804.

[11] Peshavaria, M., Larmie, B.L., Lausier, J., Satish, B., Habibovic, A., Roskens, V., et al., 2006. Regulation of pancreatic beta-cell regeneration in the normoglycemic 60% partial-pancreatectomy mouse. Diabetes 55:3289–3298.

[12] Dor, Y., Brown, J., Martinez, O.I., Melton, D.A., 2004. Adult pancreatic beta-cells are formed by self-duplication rather than stem-cell differentiation. Nature 429:41–46.

[13] van der Meulen, T., Mawla, A.M., DiGruccio, M.R., Adams, M.W., Nies, V., Dolleman, S., et al., 2017. Virgin beta cells persist throughout Life at a neogenic niche within pancreatic islets. Cell Metabolism 25:911–926 e916.

[14] Chera, S., Baronnier, D., Ghila, L., Cigliola, V., Jensen, J.N., Gu, G., et al., 2014. Diabetes recovery by age-dependent conversion of pancreatic delta-cells into insulin producers. Nature 514:503–507.

[15] Akiyama, H., Kim, J.E., Nakashima, K., Balmes, G., Iwai, N., Deng, J.M., et al., 2005. Osteo-chondroprogenitor cells are derived from Sox9 expressing precursors. Proceedings of the National Academy of Sciences of the U S A 102:14665–14670.

[16] Lynn, F.C., Smith, S.B., Wilson, M.E., Yang, K.Y., Nekrep, N., German, M.S., 2007. Sox9 coordinates a transcriptional network in pancreatic progenitor cells. Proceedings of the National Academy of Sciences of the U S A 104:10500–10505.

[17] Seymour, P.A., Freude, K.K., Tran, M.N., Mayes, E.E., Jensen, J., Kist, R., et al., 2007. SOX9 is required for maintenance of the pancreatic progenitor cell pool. Proceedings of the National Academy of Sciences of the U S A 104:1865–1870.

[18] Kopp, J.L., Dubois, C.L., Schaffer, A.E., Hao, E., Shih, H.P., Seymour, P.A., et al., 2011. Sox9+ ductal cells are multipotent progenitors throughout development but do not produce new endocrine cells in the normal or injured adult pancreas. Development 138:653–665.

[19] Seymour, P.A., 2014. Sox9: a master regulator of the pancreatic program. The Review of Diabetic Studies 11:51–83.

[20] Solar, M., Cardalda, C., Houbracken, I., Martin, M., Maestro, M.A., De Medts, N., et al., 2009. Pancreatic exocrine duct cells give rise to insulin-producing beta cells during embryogenesis but not after birth. Developmental Cell 17:849–860.

[21] Zhang, M., Lin, Q., Qi, T., Wang, T., Chen, C.C., Riggs, A.D., et al., 2016. Growth factors and medium hyperglycemia induce Sox9+ ductal cell differentiation into beta cells in mice with reversal of diabetes. Proceedings of the National Academy of Sciences of the U S A 113:650–655.

 

[22] Wang, Y.J., Kaestner, K.H., 2019. Single-cell RNA-seq of the pancreatic islets–a promise not yet fulfilled? Cell Metabolism 29:539–544.
[23] Wang, Y.J., Schug, J., Won, K.J., Liu, C., Naji, A., Avrahami, D., et al., 2016. Single-cell transcriptomics of the human endocrine pancreas. Diabetes 65: 3028–3038.
[24] Baron, M., Veres, A., Wolock, S.L., Faust, A.L., Gaujoux, R., Vetere, A., et al., 2016. A single-cell transcriptomic map of the human and mouse pancreas reveals inter- and intra-cell population structure. Cell Syst 3:346–360 e344.
[25] Muraro, M.J., Dharmadhikari, G., Grun, D., Groen, N., Dielen, T., Jansen, E., et al., 2016. A single-cell transcriptome atlas of the human pancreas. Cell Syst 3:385–394 e383.
[26] Segerstolpe, A., Palasantza, A., Eliasson, P., Andersson, E.M., Andreasson, A.C., Sun, X., et al., 2016. Single-cell transcriptome profiling of human pancreatic islets in health and type 2 diabetes. Cell Metabolism 24:593–607.
[27] Tatsuoka, H., Sakamoto, S., Yabe, D., Kabai, R., Kato, U., Okumura, T., et al., 2020. Single-cell transcriptome analysis dissects the replicating process of pancreatic beta cells in partial pancreatectomy model. iScience 23:101774.
[28] Xin, Y., Kim, J., Ni, M., Wei, Y., Okamoto, H., Lee, J., et al., 2016. Use of the Fluidigm C1 platform for RNA sequencing of single mouse pancreatic islet cells. Proceedings of the National Academy of Sciences of the U S A 113:3293–3298.
[29] Furuyama, K., Kawaguchi, Y., Akiyama, H., Horiguchi, M., Kodama, S., Kuhara, T., et al., 2011. Continuous cell supply from a Sox9-expressing progenitor zone in adult liver, exocrine pancreas and intestine. Nature Genetics 43:34–41.
[30] Soeda, T., Deng, J.M., de Crombrugghe, B., Behringer, R.R., Nakamura, T., Akiyama, H., 2010. Sox9-expressing precursors are the cellular origin of the cruciate ligament of the knee joint and the limb tendons. Genesis 48:635–644.
[31] Jaitin, D.A., Kenigsberg, E., Keren-Shaul, H., Elefant, N., Paul, F., Zaretsky, I., et al., 2014. Massively parallel single-cell RNA-seq for marker-free decomposition of tissues into cell types. Science 343:776–779.
[32] Baran, Y., Bercovich, A., Sebe-Pedros, A., Lubling, Y., Giladi, A., Chomsky, E., et al., 2019. MetaCell: analysis of single-cell RNA-seq data using K-nn graph partitions. Genome Biol 20:206.
[33] Islam, M.S., Loots du, T., 2009. Experimental rodent models of type 2 diabetes: a review. Methods & Findings in Experimental & Clinical Pharmacology 31:249–261.
[34] Bouwens, L., 2006. Beta cell regeneration. Current Diabetes Reviews 2:3–9.
[35] Keren-Shaul, H., Kenigsberg, E., Jaitin, D.A., David, E., Paul, F., Tanay, A., et al., 2019. MARS-seq2.0: an experimental and analytical pipeline for indexed sorting combined with single-cell RNA sequencing. Nature Protocols 14:1841–1862.
[36] Chen, Q., Peto, C.A., Shelton, G.D., Mizisin, A., Sawchenko, P.E., Schubert, D., 2009. Loss of modifier of cell adhesion reveals a pathway leading to axonal degeneration. Journal of Neuroscience 29:118–130.
[37] Caspi, E., Rosin-Arbesfeld, R., 2008. A novel functional screen in human cells identifies MOCA as a negative regulator of wnt signaling. Molecular Biology of the Cell 19:4660–4674.
[38] Kashiwa, A., Yoshida, H., Lee, S., Paladino, T., Liu, Y., Chen, Q., et al., 2001. Isolation and characterization of novel presenilin binding protein. Journal of Neurochemistry 75:109–116.
[39] Ferguson, L.A., Docherty, H.M., Mackenzie, A.E., Docherty, K., 2009. An engineered zinc finger protein reveals a role for the insulin VNTR in the regulation of the insulin and adjacentIGF2genes. FEBS Letters 583:3181–3186.
[40] Arrojo, E.D.R., Jacob, S., Garcia-Prieto, C.F., Zheng, X., Fukuda, M., Nhu, H.T.T., et al., 2019. Structural basis for delta cell paracrine regulation in pancreatic islets. Nature Communications 10:3700.
[41] Rorsman, P., Huising, M.O., 2018. The somatostatin-secreting pancreatic delta-cell in health and disease. Nature Reviews Endocrinology 14:404–414.
[42] Giladi, A., Cohen, M., Medaglia, C., Baran, Y., Li, B., Zada, M., et al., 2020. Dissecting cellular crosstalk by sequencing physically interacting cells. Nature Biotechnology 38:629–637.
[43] Klochendler, A., Caspi, I., Corem, N., Moran, M., Friedlich, O., Elgavish, S., et al., 2016. The genetic program of pancreatic beta-cell replication in vivo. Diabetes 65:2081–2093.
[44] Guo, S., Dai, C., Guo, M., Taylor, B., Harmon, J.S., Sander, M., et al., 2013. Inactivation of specific beta cell transcription factors in type 2 diabetes. Journal of Clinical Investigation 123:3305–3316.
[45] Zhang, C., Moriguchi, T., Kajihara, M., Esaki, R., Harada, A., Shimohata, H., et al., 2005. MafA is a key regulator of glucose-stimulated insulin secretion. Molecular and Cellular Biology 25:4969–4976.
[46] Aguayo-Mazzucato, C., Koh, A., El Khattabi, I., Li, W.C., Toschi, E., Jermendy, A., et al., 2011. Mafa expression enhances glucose-responsive insulin secretion in neonatal rat beta cells. Diabetologia 54:583–593.
[47] Kopp, J.L., von Figura, G., Mayes, E., Liu, F.F., Dubois, C.L., Morris, JPt, et al., 2012. Identification of Sox9-dependent acinar-to-ductal reprogramming as the principal mechanism for initiation of pancreatic ductal adenocarcinoma. Cancer Cell 22:737–750.
[48] Togashi, Y., Shirakawa, J., Orime, K., Kaji, M., Sakamoto, E., Tajima, K., et al., 2014. beta-Cell proliferation after a partial pancreatectomy is independent of IRS-2 in mice. Endocrinology 155:1643–1652.
[49] Teta, M., Rankin, M.M., Long, S.Y., Stein, G.M., Kushner, J.A., 2007. Growth and regeneration of adult beta cells does not involve specialized progenitors. Developmental Cell 12:817–826.
[50] Ackermann Misfeldt, A., Costa, R.H., Gannon, M., 2008. Beta-cell proliferation, but not neogenesis, following 60% partial pancreatectomy is impaired in the absence of FoxM1. Diabetes 57:3069–3077.
[51] Leiter, E.H., Gapp, D.A., Eppig, J.J., Coleman, D.L., 1979. Ultrastructural and morphometric studies of delta cells in pancreatic islets from C57BL/Ks diabetes mice. Diabetologia 17:297–309.
[52] Alan, L., Olejar, T., Cahova, M., Zelenka, J., Berkova, Z., Smetakova, M., et al., 2015. Delta cell hyperplasia in adult goto-kakizaki (GK/MolTac) diabetic rats. Journal of Diabetes Research 2015:385395.
[53] Shuai, H., Xu, Y., Yu, Q., Gylfe, E., Tengholm, A., 2016. Fluorescent protein vectors for pancreatic islet cell identification in live-cell imaging. Pflügers Archiv 468:1765–1777.
[54] Fonseca, S.G., Gromada, J., Urano, F., 2011. Endoplasmic reticulum stress and pancreatic beta-cell death. Trends in Endocrinology and Metabolism 22: 266–274.
[55] Madisen, L., Zwingman, T.A., Sunkin, S.M., Oh, S.W., Zariwala, H.A., Gu, H., et al., 2010. A robust and high-throughput Cre reporting and characterization system for the whole mouse brain. Nature Neuroscience 13:133–140.
[56] Szot, G.L., Koudria, P., Bluestone, J.A., 2007. Murine pancreatic islet isolation. Journal of Visualized Experiments, 255.
[57] Farack, L., Egozi, A., Itzkovitz, S., 2018. Single molecule approaches for studying gene regulation in metabolic tissues. Diabetes, Obesity and Metabolism 20(Suppl 2):145–156.
[58] Farack, L., Itzkovitz, S., 2020. Protocol for single-molecule fluorescence in situ hybridization for intact pancreatic tissue. STAR Protoc 1:100007.
[59] Itzkovitz, S., Lyubimova, A., Blat, I.C., Maynard, M., van Es, J., Lees, J., et al., 2011. Single-molecule transcript counting of stem-cell markers in the mouse intestine. Nature Cell Biology 14:106–114.
[60] Kim, D., Paggi, J.M., Park, C., Bennett, C., Salzberg, S.L., 2019. Graph-based genome alignment and genotyping with HISAT2 and HISAT-genotype. Nature Biotechnology 37:907–915.

 